The voltage sensitive Lc-type Ca^{2+} channel is functionally coupled to the exocytotic machinery

(exocytosis/β-cells/synaptotagmin/syntaxin/capacitance)

Ofer Wiser*, Michael Trus*, Ana Hernández*, Erik Renström†, Sebastian Barg†, Patrik Rorsman†, and Daphne Atlas*‡

*Department of Biological Chemistry, The Hebrew University of Jerusalem, Jerusalem, 91904 Israel; and †Physiological Sciences, University of Lund
Helgonavagen 5, S-223 62 Lund, Sweden

ABSTRACT Although N- and P-type Ca^{2+} channels predominant in fast-secreting systems, Lc-type Ca^{2+} channels (C-class) can play a similar role in certain secretory cells and synapses. For example, in retinal bipolar cells, Ca^{2+} entry through the Lc channels triggers ultrafast exocytosis, and in pancreatic β-cells, evoked secretion is highly sensitive to Ca^{2+}. These findings suggest that a rapidly release pool of vesicles colocalizes with the Ca^{2+} channels to allow high Ca^{2+} concentration and a tight coupling of the Lc channels at the release site. In binding studies, we show that the Lc channel is physically associated with synaptotagmin (p65) and the soluble N-ethylmaleimide-sensitive attachment proteins receptors: syntaxin and synaptosomal-associated protein of 25 kDa. Soluble N-ethylmaleimide-sensitive attachent proteins receptors coexpressed in *Xenopus* oocytes along with the Lc channel modify the kinetic properties of the channel. The modulatory action of syntaxin can be overcome by coexpressing p65, where at a certain ratio of p65/syntaxin, the channel regains its unaltered kinetic parameters. The cytosolic region of the channel, Lc$_{753–893}$, separating repeats II–III of its α1C subunit, interacts with p65 and "pulls" down native p65 from rat brain membranes. Lc$_{753–893}$ injected into single insulin-secreting β-cell, inhibits secretion in response to channel opening, but not in response to photolysis of caged Ca^{2+}, nor does it affect Ca^{2+} current. These results suggest that Lc$_{753–893}$ competes with the endogenous channel for the synaptic proteins and disrupts the spatial coupling with the secretory apparatus. The molecular organization of the Lc channel and the secretory machinery into a multiprotein complex (named excitosome) appears to be essential for an effective depolarization evoked exocytosis.

Regulated secretion in synapses occurs at a fast speed from vesicles preassembled with N- and P-type voltage sensitive Ca^{2+} channels (1). In contrast, in many neuroendocrine cells exocytosis triggered by Ca^{2+} entry through Lc channel, is slower and persists for tens of milliseconds after Ca^{2+} influx has stopped, implying that the vesicles are localized at a distance from the source of Ca^{2+} entry (2–4). Although exocytosis is slow in various endocrine cells in which secretion is mediated by Lc channel (C-class), there are reports suggesting a close association of Lc channels with the exocytotic machinery (5–8). For example a combined study of amperometry and laser imaging in chromaffin cells have shown that the sites of Ca^{2+} entry and catecholamine release are close (5, 6). Similarly, in mouse pancreatic β-cells, Lc channels have been shown to colocalize with insulin-containing secretory granules (7). Previously, we showed that the expression of syntaxin, synaptosomal-associated protein of 25 kDa (SNAP-25), and p65 along with the L- and N-type channel modify the kinetic properties of the channels (8–10). The N-type Ca^{2+} channel binds syntaxin and SNAP-25 (11–14) at a site in the cytoplasmic domain of α1B subunit (9, 10, 15, 16) and is physiologically associated within release sites (17–20). Colocalization of the N channel with the exocytotic machinery was inferred from disruption of the release process in cells injected with the interacting domain of the channel (21, 22). Although the speed of the release process in neuroendocrine cells is slower than in neuronal cell (23), Lc channels, like N channels, appear to associate with synaptic proteins. Indeed, an ultrafast exocytosis, which would require a close association of the channel with the exocytotic machinery, was described in retinal bipolar neuron (24). In these cells, a fast secretion, similar in rate to fast release in neuronal secretion, is triggered by L-type Ca^{2+} channels (25). The tight temporal and focal regulation of fast secretion in bipolar cells infers an organization and interaction of the Lc channel with the exocytotic machinery, similar to that observed for N channels in fast synapses.

The molecular organization of the Lc channel with synaptic proteins was investigated in a combined biochemical and physiological approach. First, in binding assays, we looked for a physical link between the Lc channel with syntaxin, SNAP-25 and p65. Second, functional interaction of the channel with the individual proteins and their assembly into a functional complex was studied by using the *Xenopus* oocytes expression system. Third, the consequence of these interactions was investigated by capacitance measurements of insulin release in single β-cells injected with the channel-interacting domain. Our results provide a molecular and functional basis to suggest the formation of a multiprotein complex (excitosome) composed of the Lc channel, p65, and soluble N-ethylmaleimide-sensitive attachment proteins receptors, which allows temporal and spatial coupling of the channel to the exocytotic vesicles.

MATERIALS AND METHODS

Constructs of Glutathione *S*-Transferase (GST) and His$_6$-Tagged Fusion Proteins. A clone carrying part of the α1C subunit was obtained by screening of a λgt11 cDNA library of PC12 cells (26). The *Bst*XI (3010) to *Pst*I (3430) fragment comprising the cytoplasmic domain (Lc$_{753–893}$) was excised and ligated into the *Sma*I site of vector QE32 (Qiagen). Lc753–779 was prepared by ligating *Bst*XI (3010)–*Msc*I (3088) fragment into the *SMAI* site in QE 30 (Qiagen). The basepair numbers

---

Abbreviations: SNAP-25, synaptosomal-associated protein of 25 kDa; GST, glutathione *S*-transferase; GSH, glutathione; τact, activation time constant.
‡To whom reprint requests should be addressed. e-mail: daphnea@leonardo.ls.huji.ac.il.
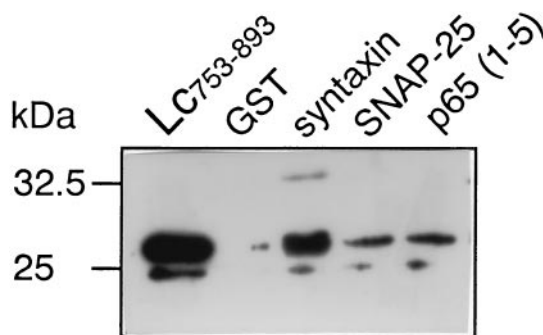
FIG. 1. Lc$_{753-893}$ binding to synaptic proteins. GST fusion proteins (100 pmol) were immobilized on GSH-agarose beads and incubated for 60 min with His$_6$ Lc$_{753-893}$ (250 pmol). After extensive washing, the remaining bound proteins were eluted with 15 mM GSH, separated on a 10% SDS acrylamide gel, transferred to nitrocellulose, and subjected to Western analysis by using anti L-peptide antibodies and ECL detection. His$_6$ Lc$_{753-893}$ (30 ng) was used as a marker.

were according to GenBank accession no. M67516 (rat brain calcium channel α-1 subunit). GST fusion proteins of SNAP-25, syntaxin, p65(1–5), p65(1–3), and p65(3–5) were gifts (see *Acknowledgment*). Constructs were transformed into the protease-deficient strain *Escherichia coli* BL21pLysS (Novagen).

Purification of His$_6$-Tagged Fusion Proteins. Bacterial pellets were thawed in the presence of 8 M urea, 150 mM NaCl, 50 mM Tris·HCl (pH 8.0), and 1% Triton X-100 and applied to nickel-nitrilotriacetic acid agarose beads. The beads were subjected to a decreasing gradient of urea, 8–0 M and washed with 150 mM NaCl, 50 mM Mes buffer, pH 6.0. After elution with 0.3 M imidazole (pH 7.0), the eluate was dialyzed against PBS. The purified protein was detected by Coomassie blue and Western analysis by using affinity-purified antibodies raised against the L-peptide TTKINMDDLQPSENEDKS and the N-peptide RHHRHRDRDKTSAST (9).

***In Vitro*-Binding Assays and Western Blotting.** Lc$_{753-893}$ (250 pmol) was bound to GST fusion proteins (100 pmol) immobilized to glutathione (GSH)-agarose 4B beads (25 μl; Sigma)
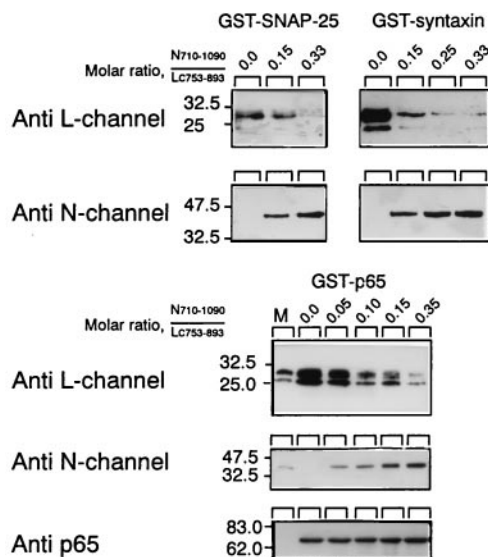

FIG. 2. Competition of Lc$_{753-893}$ and N-Loop$_{710-1090}$ for synaptic proteins. His$_6$Lc$_{753-893}$ fusion protein (0.5 μM; 2.5 μg) was bound to synaptic proteins immobilized on GSH-agarose beads with increasing N-Loop$_{710-1090}$ concentration as indicated. The proteins were transferred to nitrocellulose and then subjected to Western analysis by using anti-L-peptide antibodies. The blots were then stripped and exposed to anti-N-peptide antibodies. A third exposure to anti-p65 antibodies shows equal amounts of GST fusion proteins, shown for GST-p65 (*Lower*).
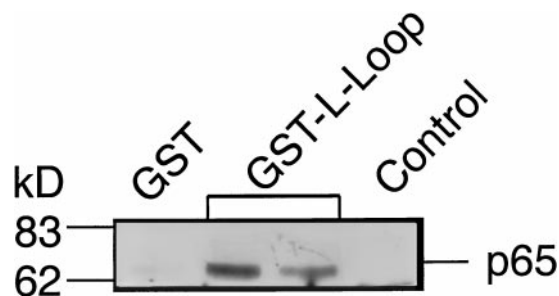

FIG. 3. L-Loop binds to p65 in rat brain lysate. GST (first lane), GST-Lc$_{753-893}$ fusion protein (10 μg) immobilized on GSH-agarose beads (second and third lanes), and GST-Lc$_{753-893}$ in solution (fourth lane) were incubated with 1% Triton X-100 lysate of rat brain membrane (1 mg) for 12 hr at 4°C. Beads were eluted with GSH, and proteins were separated on SDS/PAGE gel (10%) and were analyzed for p65 by immunoblotting (see Fig. 1) by using anti-p65 antibodies.

in PBS with Tween 20 (PBST) buffer (mM): 140 NaCl, 2.7 KCl, 10.1 Na$_2$HPO$_4$, 1.8 Na$_3$PO$_4$, and 0.05% Tween 20, pH 7.3.
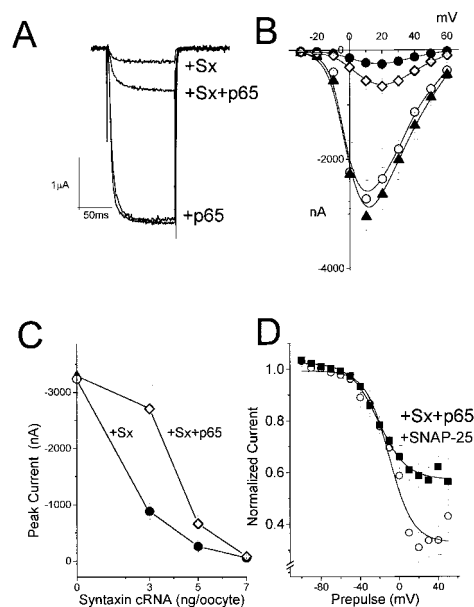

FIG. 4. Interaction of syntaxin and p65 with Lc channels expressed in *Xenopus* oocytes. Lc channel subunits α*1C/α2δ/β2A were expressed in *Xenopus* oocytes either alone or in combination with synaptic protein, as indicated. Inward Ba^{2+} currents were evoked from a holding potential of −80 mV in response to a 500 ms pulse to various test potentials in 10 mV increments and are presented as a current-voltage relationship. (*A*) Superposition of macroscopic currents evoked to +20 mV. (*B*) Leak-subtracted peak currents from oocytes expressing the three channel subunits (○), with syntaxin 1A (5 ng/oocytes ●), p65 (5 ng; △), and both combined (◇). (*C*) Recovery of inward currents in oocytes expressing Lc channel subunits with syntaxin and p65 as a function of injected syntaxin cRNA. The channel subunits were injected 1 day before injection of syntaxin 1A and p65. Inward currents in oocytes expressing the channel alone (○), with syntaxin (●), and in the presence of p65 (5 ng; ◇) represent three different sets of experiments. The data points correspond to the mean ± SEM of currents (n = 6–9) at each experimental point. Two-sample Student's *t* tests assuming unequal variance were applied, and *P* values < 0.01 were obtained. (*D*) Inactivation curves of steady–state normalized Ba^{2+} currents, generated by Lc channel subunits (○), with p65, syntaxin 1A, and SNAP-25 (■). Peak normalized currents were fitted to a Boltzmann inactivation curve represented by the smooth curve (8). Oocytes were injected with 1,2-bis(2-aminophenoxy)ethane-*N,N,N',N'*-tetraacetate (BAPTA) to a final concentration of 60 min before recording. The data points correspond to the mean ± SEM of currents (n = 7). cRNA injected (per oocyte): 2 ng α*1C, 1.5 ng α2δ, and 5 ng β2A.
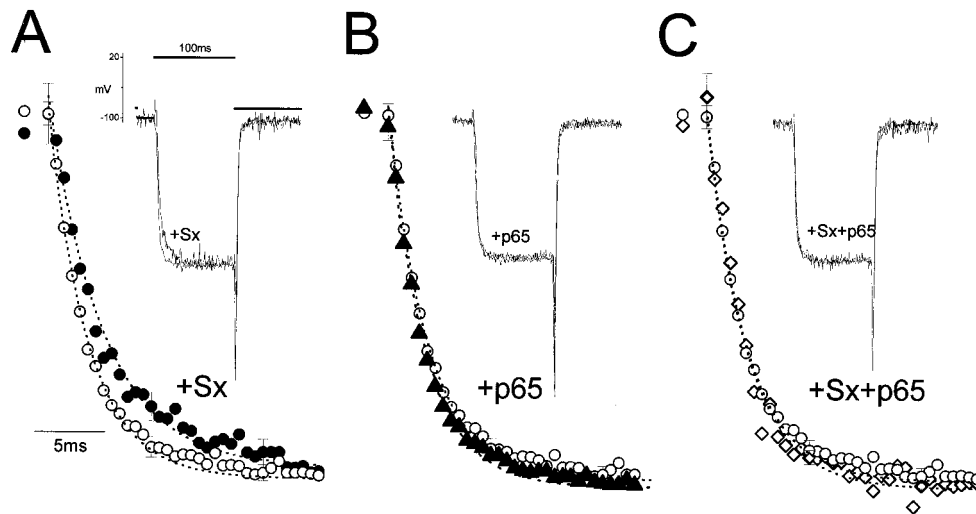
FIG. 5.   The activation kinetics of the Lc-type channel is modified by syntaxin and p65. Rates of activation of the Lc channels (τact = 3.9 $\pm$ 0.8 ms; $\bigcirc$; n = 16) were recorded in oocytes expressing syntaxin (Sx) (*A*) (7 ng/oocyte; τact = 6.2 $\pm$ 1.5; $\bullet$; n = 8), p65 (*B*) (5 ng/oocyte; τact = 4.0 $\pm$ 0.5 ms; $\triangle$; n = 12), and p65 (7 ng) and syntaxin (*C*) (5 ng/oocyte; τact = 4.1 $\pm$ 0.8 ms; $\diamondsuit$; n = 10). Ba^{2+} currents were evoked from a holding potential of -80 mV in response to a 100-ms pulse to a test potential of $+20$ mV. (*Insets*) Leak-subtracted representative traces (on-line subtraction). The dotted lines represent mono-exponential fitting of the normalized traces. Statistical significance was determined by using one-way ANOVA $P < 1.7$E-8.

After 1 hr at room temperature in PBS buffer containing 1 mg/ml BSA, the beads were washed three times with 1 ml of PBS containing 0.1% Triton X-100, and bound proteins were eluted with 15 mM GSH. Proteins were separated on SDS/ PAGE, transferred to nitrocellulose, and probed by using affinity-purified antibodies generated against the Lc peptide, detected by enhanced chemiluminescence. Pull-down experiments were carried out by immobilized GST and GST-Lc$_{753-893}$ (10 μg), added to a 1% Triton X-100 lysate of rat brain membrane (1 mg) and incubated for 12 hr at 4°C. Beads were washed three times with 1 ml of PBST buffer, were eluted, and were analyzed for p65 (see above).

cRNA Injection and Protein Expression in *Xenopus* Oocytes. Stage V–VI oocytes were removed surgically from the ovaries of anesthetized animals and transferred to a Ca^{2+}-free ND96 solution (mM): 96 NaCl, 2 KCl, 1 MgCl$_2$, 5 Hepes (pH 7.4), containing 2 mg/ml collagenase (154 units/mg, Worthington). The follicular cell layer was removed and the oocytes were then washed extensively and placed into a ND96 solution containing 1.8 CaCl$_2$, 2.5 mM sodium pyruvate, 100 units/ml penicillin, and 100 μg/ml streptomycin at 20°C for 12–20 h before cRNA injection. Plasmid DNA for the channel subunits, α*1C, α2δ, β2A syntaxin 1A, SNAP-25, and p65 (8) were linearized, treated with proteinase K, and transcribed with T7 polymerase and *in vitro* transcription kit (Stratagene) in the presence of the cap analog G (5′) ppp(5′)G (Pharmacia). The *in vitro*-transcribed capped cRNAs were injected in a final volume of 40 nl.

Electrophysiological Assays in *Xenopus* Oocytes. Whole cell currents were recorded by applying a standard two-microelectrode voltage clamp by using a Dagan 8500 amplifier (Dagan Instruments, Minneapolis) (8). Voltage and current agar-cushioned electrodes (0.3- to 0.6-mΩ tip resistance) were filled with 3 M KCl. Current-voltage relationships were determined by voltage steps from -80 to $+60$ mV of 500 ms duration, with 30 sec intervals, in Ba^{2+} solution (in mM): 40 Ba(OH)$_2$, 50 N-methyl D-glucamine, 1 KOH, and 5 Hepes (pH 7.5), titrated to pH 7.5 [(CH$_3$)$_2$SO$_4$].

Voltage-dependent inactivation was carried out as described (8) and fitted by a single Boltzmann distribution with normalized current = C/{1 + exp[($V_{1/2}$ − V_m)/k]} + (1 − C), the current observed following a conditioning pulse to a membrane potential V_m, $V_{1/2}$ the midpoint of inactivation, k the

slope parameter. Activation kinetics were determined by using 100 ms leak subtracted pulses to $+20$ mV. Current traces were analyzed by a mono-exponential fit of the PCLAMP6 software (Axon Instruments, Foster City, Ca).

Patch-Clamp Recordings from β-cells. Pancreatic islets of NMRI mice were isolated by collagenase digestion, dispersed into single cells, and maintained in tissue culture for up to 2 days. Exocytosis was detected as changes in cell capacitance by using Sylgard-coated, fire-polished capillaries (2- to 4-MΩ tip resistance) with EPC-7 amplifier and PULSE software (version 8.02, HEKA Electronics, Lambrecht/Pfalz, Germany). Final temporal resolution was set to 2 ms.

Exocytosis was elicited by single 500-ms voltage-clamp depolarization from the holding potential -70–0 mV. After establishment of whole-cell configuration, the pipette solution was dialyzed into the cell for 3 min before stimulation to ensure wash-in of Lc$_{753-893}$. Ca^{2+} current-voltage relationships (I–V) were determined by 300 ms depolarization applied at $\approx$10 s interval, from holding potential -70 mV to voltages between -50 and $+50$ mV (10 mV increment). The integrated Ca^{2+} current during the entire depolarization and the time course of inactivation were determined by using the software PULSEFIT (version 8.02, Heka Electronics).

Photorelease of Caged Ca^{2+}. Photolysis of Ca^{2+} nitrophenyl–EGTA complex was effected by brief UV light flashes (<2 ms; XF-10, HiTech, UK). [Ca^{2+}]$_i$ increase was measured by dual-wavelength spectrofluorimetry by using Ca^{2+} indicator BTC (10 μM; Molecular Probes). [Ca^{2+}]$_i$ was calculated by using K_D = 15.2 μM for the Ca^{2+}–BTC complex in the presence of Mg^{2+} (27).

Patch-Clamp Solutions. Flash photolysis of caged Ca^{2+} (mM): 138 NaCl, 5.6 KCl, 1.2 MgCl$_2$, 2.6 CaCl$_2$, 5 D-glucose, and 5 Hepes, pH 7.4 (NaOH). In all other experiments, 20 mM of NaCl was equimolarly replaced by tetraethylammonium chloride. Single voltage-clamp depolarization, electrode solution (mM): 125 Cs-glutamate, 15.6 NaCl, 10 CsCl, 1 MgCl$_2$, 0.1 KCl, 0.4 NaH$_2$PO$_4$, 0.07 KH$_2$PO$_4$, 5 Hepes, 0.05 EGTA, 0.1 cAMP, and 3 Mg-ATP, pH 7.15 (CsOH). The pipette solution was dialyzed for 3 min before stimulation because it was demonstrated to be sufficient for wash-in the macromolecule into the cytosol, using dextran-conjugated fura-2, 30 kDa (C. Ämmälä and P.R., unpublished data). For I–V relationships, 10 mM CaCl$_2$ was added to the extracellular solution, and the

intracellular solution was the same as that used for cell capacitance except for 10 mM EGTA.

RESULTS

Lc Channel Binding to Synaptic Proteins. To determine L-type channel binding to synaptic proteins, we performed *in vitro* studies by using recombinant fusion proteins. The most likely interaction site for Lc-type channel is the cytoplasmic domain separating repeats II and III of the channel $\alpha 1C$ subunit, as previously described for the $\alpha 1B$ of the N-type channel (9, 10, 15, 16).

The cytosolic domains of syntaxin 1A, SNAP-25, and p65 in a form of GST fusion proteins, immobilized to GSH-agarose beads, were incubated with equimolar concentration of the II–III L-loop (His6-Lc$_{753-893}$; 0.5 μM; 2.5 μg). Binding of Lc$_{753-893}$ was determined by immunoblot by using anti L-peptide antibodies. As shown in Fig. 1, Lc$_{753-893}$ specifically binds to syntaxin, SNAP-25 and p65, in contrast to corresponding region of the skeletal Ls-type channel, Ls$_{670-800}$ (15). A smaller peptide Lc$_{753-779}$ bound to neither of these proteins (data not shown).

The specificity of Lc$_{753-893}$ interaction was evaluated further by competition with the II–III domain of the N channel, previously reported to interact with the synaptic proteins (9, 10, 15, 16). In this experiment, Lc$_{753-893}$ binding was carried out in the presence of increasing concentrations of N-Loop$_{710-1090}$ (Fig. 2). As the concentration of the competing N-loop increased, there was a significant decrease in the amount of bound Lc$_{753-893}$ (Fig. 2 *Upper*) and an increase of N-Loop$_{710-1090}$ (Fig. 2 *Lower*). N-Loop$_{710-1090}$ displayed a higher affinity (>5 fold) for the three synaptic proteins. At a molar ratio of N-Loop$_{710-1090}$/Lc$_{753-893}$ <0.2, Lc$_{753-893}$ binding was reduced to <10% the amount when no competitor was present (Fig. 2). To confirm a selective Lc$_{753-893}$ interaction with synaptic protein under more physiological conditions, we used the "pull down" assay. As shown in Fig. 3, GST-Lc$_{753-893}$ "pulled" down p65 from the brain lysate, whereas no p65 was bound either to immobilized GST or to beads-free Lc$_{753-893}$.

Functional Interaction of the Lc Channel with Synaptic Proteins. To test for syntaxin and p65 modulation of Lc channels, *Xenopus* oocytes were injected with cRNA encoding syntaxin 1A, p65, and channel subunits α^*1C, $\beta 2A$, and $\alpha 2\delta$. Expressed current could be totally blocked by 0.1 μM nifedipine (data not shown). Although the syntaxin (7 ng/oocyte) inhibitory effect on current amplitude was seen at all voltages [Fig. 4; (8)], p65 (5 ng/oocyte) had virtually no effect on the current (Fig. 4 *A–C*). When syntaxin and p65 were coexpressed, p65 tended to reverse the syntaxin inhibitory action. Because syntaxin binds strongly to p65 (28–29), changes in the kinetic properties of the channel were monitored by altering the syntaxin/p65 ratio. Indeed, decreasing amounts of syntaxin cRNA resulted in a progressively smaller inhibition of current amplitude (75% decrease for 3 ng/oocyte of cRNA, 85% for 5 ng, 95% for 7 ng; Fig. 4*C*) and an increase in p65 ability to restore current amplitude.

Although syntaxin and p65 alone marginally affected the steady–state voltage inactivation curves (not shown), syntaxin, SNAP-25, and p65 combined shifted the Boltzmann curve of the channel from $V_{1/2} = -10.5 \pm 2.8$ to -21 ± 1.4 mV (Fig. 4*D*). The effects of syntaxin and p65 on the activation kinetics of the Lc channel were tested as well. The activation time constant (τact) of the Lc channel was notably affected by syntaxin (Fig. 5*A*). On its own, p65 did not modify τact (τact = 4.0 $\pm$ 0.8 ms for the channel alone, 4.0 $\pm$ 0.55 ms for the channel with p65), but it canceled the syntaxin effect τact = 6.2 $\pm$ 1.47 ms to τact = 4.17 $\pm$ 0.8 ms (Fig. 5 *B* and *C*). Rise time analysis showed the same effects of syntaxin and syntaxin/p65. The rise time value measured for the Lc channel was similar to that previously reported (30).

Disrupting Lc Channel Interaction with the Exocytotic Machinery. Lc$_{753-893}$ effect on exocytosis was measured as the increase in cell capacitance, evoked by 500-ms voltage-clamp depolarization (Fig. 6). Under control conditions, depolarization produced an increase in cell capacitance ≈100 fF (Fig. 6 *A* and *B*). When Lc$_{753-893}$ (10 μM) was added into the pipette solution, depolarization failed to evoke exocytosis, whereas Lc$_{753-779}$ (10 μM) had no significant effect (Fig. 6 *A* and *B*). On average, the increase in cell capacitance elicited to 0 mV was 105 $\pm$ 22 fF ($n = 16$) in control, 5 $\pm$ 2 fF ($n = 16$) in Lc$_{753-893}$ and 83 $\pm$ 34 fF ($n = 6$) in Lc$_{753-779}$ (not significantly different from control but $P < 0.001$ compared with values in the presence of Lc$_{753-893}$; Fig. 6*B*).

To ascertain that suppression of exocytosis cannot simply be attributed to Lc$_{753-893}$ interference with Ca^{2+} entry, Ca^{2+} currents were elicited by voltage-clamp depolarization in the presence of Lc$_{753-893}$ (Fig. 6 *C* and *D*). Ca^{2+} currents activated
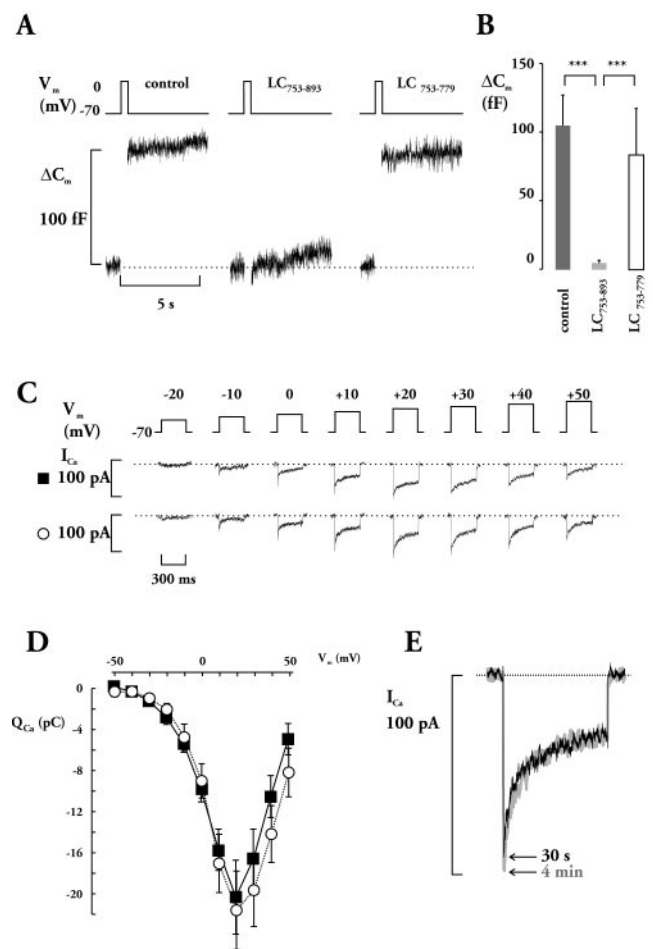

FIG. 6. Effect of L-loop on depolarization-evoked exocytosis in β-cells. (*A*) Changes in membrane capacitance (ΔC_m) elicited by 500 ms of depolarization under control conditions and after inclusion of the peptides in the pipette solution as indicated. The dotted horizontal line indicates the prestimulatory capacitance level. (*B*) Histograms summarizing the Lc$_{753-893}$ and Lc$_{753-779}$ effects on depolarization-induced exocytosis. Values are mean values $\pm$ SEM of 16 (control and Lc$_{753-893}$) and six experiments (Lc$_{753-779}$), respectively. Statistical significance was calculated by using Student's *t* test and the asterisks indicate $P < 0.001$. (*C*) Ca^{2+} currents elicited by 300-ms depolarization pulses to the indicated potentials in the absence (▼) or presence (○) of Lc$_{753-893}$. (*D*) Voltage dependence of integrated Ca^{2+} currents (Qca). The traces represent mean values $\pm$ SEM of seven and six experiments in the absence (■ solid line) or presence (○ dotted line) of Lc$_{753-893}$, respectively. (*E*) Ca^{2+} currents recorded in response to +10 mV (to facilitate analysis of inactivation) 30 s (black) and 4 min (gray) after establishment of the whole cell configuration.
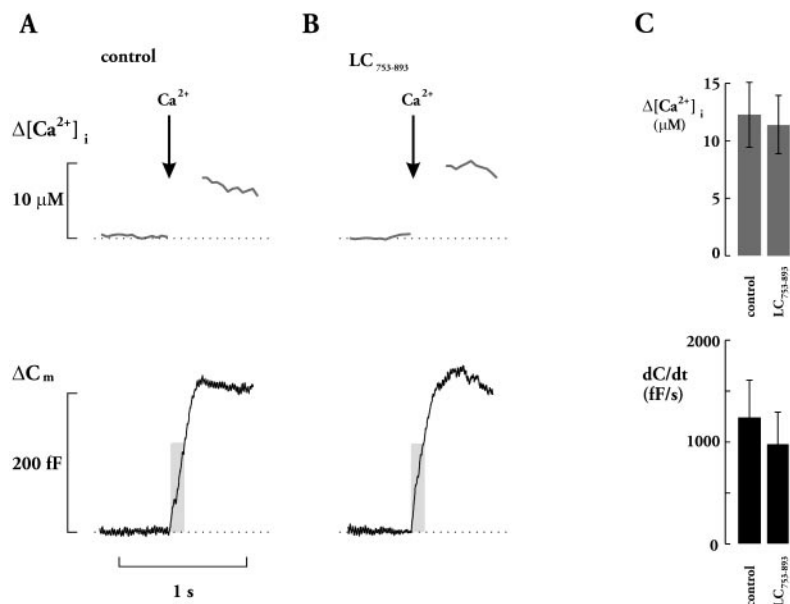
Fig. 7. L-loop does not prevent exocytosis elicited by photolysis of caged Ca^{2+} in β-cells. Increases in $[Ca^{2+}]_i$ and cell capacitance (ΔC_m) after photolysis of Ca^{2+} nitrophenyl-EGTA, in the absence (*A*) or presence (*B*) of 10 μM $Lc_{753-893}$. The arrows indicate the time at which photolysis was effected by UV light flashes. The shaded areas highlight the period (first 100 ms after the flash) used to determine the initial rate (dC/dt) of exocytosis. The dotted horizontal lines indicate the prestimulatory levels. (*C*) Histograms summarizing the $Lc_{753-893}$ effect on $[Ca^{2+}]_i$ rise ($\Delta[Ca^{2+}]_i$) and initial rate of exocytosis (dC/dt). Data are presented as mean values $\pm$ SEM of 11 experiments in each group.

at voltages more positive than -50 mV, peaked at $+20$ mV and decreased at more positive membrane potential, indicating a reversal at a voltage beyond $+60$ mV. The integrated Ca^{2+} currents (0 mV) averaged 9.9 ± 1.2 ($n = 7$) and 9.0 ± 1.7 pC ($n = 6$) in the absence and presence of $Lc_{753-893}$, respectively. Such a small decrease in Ca^{2+} currents is insufficient to account for the dramatic effect on secretion (31). During depolarization, there was a time dependent decline in Ca^{2+} current amplitude that we attribute to Ca^{2+}-dependent inactivation of the Ca^{2+} channels rather then activation of a delayed outward current. The latter conclusion is suggested by the close correlation between Ca^{2+} current amplitude and changes of $[Ca^{2+}]_i$ (7, 32). Ca^{2+} current inactivation can be described as the sum of two exponential functions: one rapid (time constant 7 ms) comprising 70% of the current and a slow (time constant >500 ms) accounting for the remaining 30%. The inactivation was not affected by the addition of $Lc_{753-893}$, and no time-dependent changes of the amplitude and kinetics were observed when comparing current responses 30 s and 4 min after the establishment of the whole-cell configuration and infusion of the peptide (Fig. 6*E*). In contrast to the strong inhibitory action on depolarization-evoked exocytosis, $Lc_{753-893}$ had no effect on secretion elicited by Ca^{2+} from photolabile Ca^{2+} chelator, nitrophenyl-EGTA (Fig. 7*A*). In the presence of $Lc_{753-893}$, elevation of $[Ca^{2+}]_i$ by ≈ 10 μM elicited a prompt increase in cell capacitance, which reached a plateau after ≈ 300 ms, similar to control (Fig. 7*B*). Average increase in $[Ca^{2+}]_i$ was 14.5 ± 3.2 and 12.0 ± 2.7 μM, in the absence and presence of $Lc_{753-893}$, respectively (Fig. 7*C Upper*). Initial rate of exocytosis [dC/dt; during the first 100 ms after the flash, when the influence of endocytosis is negligible (27)] was 1250 ± 369 and 980 ± 280 fF/s in the absence and presence of $Lc_{753-893}$, respectively (Fig. 7*C Lower*).

DISCUSSION

Recent findings provide considerable evidence for a close association of presynaptic N-type channels and transmitter release site. The two-way cross talk enables a tightly controlled process that is characteristic of the neuronal cell. In the present

study we investigated whether these interactions prevail in neuroendocrine cells, at which Lc channels trigger secretion.

Direct Binding of Synaptic Proteins to the Cytosolic Domain of the Lc Channel. Our results show that syntaxin 1A, SNAP-25 and p65 specifically interact with the Lc channel at the II–III loop of the $\alpha 1C$ subunit ($Lc_{753-893}$). The distinct N-Loop/L-Loop competition, consistent with a specific $Lc_{753-893}$ interaction, provides strong evidence for a common recognition site shared by the two type channels. The apparent lower affinity of $Lc_{753-893}$, the cytosolic domain of the Lc channel, for the synaptic proteins as compared with N-Loop$_{710-1090}$, indicate perhaps, important differences between secretion in neuroendocrine and neuronal cells, and may in part, explain why the latter are the predominant release-gating channel in nerve terminals that have both L- and N-type channels. The "pull down" experiments suggest that also *in vivo*, the vesicle associates with the channel at the II–III domain.

Functional Interaction of the Lc Channel with Syntaxin, SNAP-25 and p65. Previous functional studies have shown that the N channel interacts simultaneously with syntaxin (8–10, 33) and p65, to form ternary and quaternary complexes (9, 10). Here, we show that although syntaxin strongly reduces and p65 has virtually no effect on current amplitude, it is restored by increasing p65/syntaxin ratio. The *in vivo* interplay of the full-length proteins expressed in *Xenopus* oocytes suggests that both syntaxin and p65 can acquire a rate-limiting role in the release process. Indeed, interference with p65 levels, by gene disruption (review 34), antibody (35) or C2 domain (36) inhibits secretion. Rescue of current amplitude by p65 discloses a delicate balance between the two synaptic proteins and could provide in part, an explanation for the above mentioned studies. Furthermore, if these findings are applicable to neuroendocrine cells, it appears that Ca^{2+} entry through Lc channels would be prevented by the abundant syntaxin, similar to the N channel (8–10). This inhibition is relieved following the binding of the vesicle to the channel (9, 10). The resumed Ca^{2+} flow would participate in the fusion process now, when the channel is in a physical and functional contact with the vesicle.

Putative binary and ternary complexes (9–12, 27, 37–40) that interact with N channel (8–14, 41) appear to interact also

with the Lc channel. Significant changes in the voltage-dependent steady–state inactivation of the Lc channel by additionally expressing SNAP-25, further support the formation of a multiprotein excitosome complex, comparable with a complex generated between p65 and the soluble N-ethylmaleimide-sensitive attachment proteins receptors with the N channel (9–10). The previously described association of synaptobrevin (38–40) to the total soluble N-ethylmaleimide-sensitive attachment proteins receptors complex makes it likely that this protein might also play a role in the function of the excitosome. Reduction in rate of activation by syntaxin and restitution to normal value by p65 confirms a three-way cross talk of the channel with the two proteins. Moreover, a slower rate of activation within the time frame of evoked release suggests that the interaction may be pertinent to the release process.

The II–III L-Loop Suppresses Depolarization-Evoked Secretion in Insulin Secreting Cells by Extending Distance Between Point of Ca^{2+} Entry and the Ca^{2+} Sensing Site. The physiological consequences of Lc channel interaction with the exocytotic core complex were explored by injecting Lc$_{753-893}$ into pancreatic β-cells. Lc$_{753-893}$ suppressed depolarization-evoked exocytosis and did not affect Ca^{2+} current amplitude, consistent with interference of a channel/synaptic proteins interaction rather than Ca^{2+} entry. The possibility that the peptides have acted by preventing synaptic protein interactions required for Ca^{2+}-dependent secretion seems rather unlikely, since Lc$_{753-893}$ did not suppress exocytosis elicited by photorelease of caged Ca^{2+}. Exocytosis in β-cells is operational at high Ca^{2+} levels (42) where half-maximal rate (20 μM) is likely to occur just beneath the inner mouth of the channel (7). We propose that Lc$_{753-893}$ binds to synaptic proteins and displaces Ca^{2+} channels from the release site. The secretory granules, now spatially removed from the inner mouth of the channel, cannot participate in secretion. This proposal is compatible with the observation that exocytosis can be elicited in the presence of Lc$_{753-893}$ by photorelease of caged Ca^{2+} (Fig. 7) or a train of depolarization (not shown) in which there is a global rather than a localized [Ca^{2+}]$_i$ increase. It appears that single Ca^{+2} channels can create individual Ca^{2+} domains, each of which is essential to activate secretion. Previous studies showed that II–III N-Loop peptide (synprint) inhibits fast synchronous synaptic transmission (21, 22). The complete inhibition of exocytosis in β-cells may indicate that secretion in these cells is equally dependent on a close physical link between Lc channels and secretory granules. Formation of the excitosome is essential for evoked release, demonstrating that the Lc channel is an integral part of the exocytotic process. Finally, despite slower kinetics of release in neuroendocrine cells (but see ref. 43), the remarkable conservation of synaptic protein interactions with L-, N- and P/Q-type Ca^{2+} channels suggests that exocytosis in neuroendocrine and neuronal cells share important aspects of regulation and spatial organization.

1. Stanley, E. F. (1997) *Trends Neurosci.* **20,** 404–409.
2. von Rüden, L. & Neher, E. (1993) *Science* **262,** 1061–1065.
3. Chow, R. H., Klingauf, J. & Neher, E. (1994) *Proc. Natl. Acad. Sci. USA* **91,** 12765–12769.
4. Chow, R. H., Klingauf, J. Heinemann, C., Zucker, R. S. & Neher, E. (1996) *Neuron* **16,** 369–376.
5. Monck, J. R., Robinson, I. M., Escobar, A. L., Vergara, J. L. & Fernandez, J. M. (1994) *Biophys. J.* **67,** 505–514.
6. Robinson, M., Finnegan, J. M., Monck, J. R., Wightman, R. M. & Fernandez, J. M. (1995) *Proc. Natl. Acad. Sci. USA* **92,** 2472–2478.
7. Bokvist, K., Eliasson, L., Ammälä, C., Renström, E. & Rorsman, P. (1995) *EMBO J.* **14,** 50–57.
8. Wiser, O., Bennett, M. K. & Atlas, D. (1996) *EMBO J.* **15,** 4100–4110.
9. Wiser, O., Tobi, D., Trus, M. & Atlas, D. (1997) *FEBS Lett.* **404,** 203–207.
10. Tobi, D., Wiser, O., Trus, M. & Atlas, D. (1998) *Receptors and Channels* **6,** 89–98.
11. Morita, T., Mori, H., Sakimura, K., Mishina, M., Sekine, Y., Tsugita, A., Odani, S., Horikawa, H. P. M., Saisu, H. & Abe, T. (1992) *Biomed. Res.* **13,** 35–40.
12. Bennett, M. K., Calakos, N. & Scheller, R. H. (1992) *Science* **257,** 255–259.
13. Yoshida, A., Oho, C., Omori, A., Kuwahara, R., Ito, T. & Takahashi, M. (1992) *J. Biol. Chem.* **267,** 24295–24928.
14. Lévêque, C., El Far, O., Martin-Moutot, N., Sato, K., Kato, R., Takahashi, R. & Seagar, M. J. (1994) *J. Biol. Chem.* **269,** 6306–6312.
15. Sheng, Zu-H., Rettig, J., Takahashi, M. & Catterall, W. A. (1994) *Neuron* **13,** 1303–1313.
16. Sheng, Zu-H., Rettig, J., Cook, T. & Catterall, W. A. (1996) *Nature (London)* **379,** 451–454.
17. Robitaille, E., Adler, E. M. & Charlton, M. P. (1990) *Neuron* **5,** 773–779.
18. Llinas, R., Sugimori, M. & Silver, R. B. (1992) *Science* **256,** 677–679.
19. Stanley, E. F. (1993) *Neuron* **11,** 1007–1011.
20. Haydon, P. G., Henderson, E. & Stanley, E. F. (1994) *Neuron* **13,** 1275–1280.
21. Mochida, S., Sheng, Zu-H., Baker, C., Kobayashi, H. & Catterall, W. A. (1996) *Neuron* **17,** 781–788.
22. Rettig, J., Heinemann, C., Asheri, U., Sheng, Zu-H, Yokoyama, C. T., Catterall, W. A. & Neher, E. (1997) *J. Neurosci.* **17,** 6647–6656.
23. Augustine, G. J. & Neher, E. (1992) *J. Physiol. (London)* **450,** 247–271.
24. von-Gersdorff, H., Vardi, E., Matthews, G. & Sterling, P. (1996) *Neuron* **16,** 1221–1227.
25. Mennerick, S. & Matthews, G. (1996) *Neuron* **17,** 1241–1249.
26. Avidor, B., Avidor, T., Schwartz, L., De Jongh, K. S. & Atlas, D. (1994) *FEBS Lett.* **342,** 209–213.
27. Eliasson, L., Renström, E., Ding, W.-G., Proks, P. & Rorsman, P. (1997) *J. Physiol. (London)* **503,** 399–412.
28. Li, C., Ullrich, J. Z., Anderson, R. G. W., Brose, N. & Südhof, T. C. (1995) *Nature (London)* **375,** 594–599.
29. Kee, Y. & Scheller, R. H. (1996) *J. Neurosci.* **16,** 1975–1981.
30. Singer, D., Biel, M., Lotan, I., Flockerzi, V., Hofmann, F. & Dascal, N. (1991) *Science* **253,** 1553–1557.
31. Renström, E., Eliasson, L., Bokvist, K. & Rorsman, P. (1996) *J. Physiol. (London)* **494,** 41–52.
32. Plant, T. D. (1988) *J. Physiol. (London)* **404,** 731–747.
33. Bezprozvanny, I., Scheller, R. H. & Tsien, R. W. (1995) *Nature (London)* **378,** 623–626.
34. Wu, M. N. & Bellen, H. J. (1997) *Curr. Opin. Neurobiol.* **7,** 624–630.
35. Elferink, L. A., Peterson, M. R. & Scheller, R. H. (1993) *Cell* **72,** 153–159.
36. Bommert, K., Charlton, M. P., DeBello, W. M., Chin, G. J., Betz, H. & Augustine, G. J. (1993) *Nature (London)* **363,** 163–165.
37. Saisu, H., Ibaraki, K., Yamaguchi, T., Sekine, Y. & Abe, T. (1991) *Biochem. Biophys. Res. Commun.* **181,** 346–350.
38. Hayashi, T., McMahon, H., Yamasaki, S., Binz, T., Hata, Y., Sudhof, T. C. & Niemann H. (1994) *EMBO J.* **13,** 5051–5061.
39. Chapman, E. R., Hanson, P. I., An, S. & Jahn, R. (1995) *J. Biol. Chem.* **270,** 23667–23671.
40. Pellegrini, L. L., O'Connor, V., Lottspeich, F. & Betz, H. (1995) *EMBO J.* **14,** 4705–4713.
41. Sheng, Zu-H., Yokoyama, C. T. & Catterall, W. A. (1997) *Proc. Natl. Acad. Sci. USA* **94,** 5405–5410.
42. Takahashi, N., Kadowaki, T., Yazaki, Y., Miyashita, Y. & Kasai, H. (1997) *J. Cell Biol.* **138,** 55–64.
43. Elhamdani, A., Zhou, Z. & Artalejo, C. R. (1998) *J. Neurosci.* **18,** 6230–6240.